**ELKOMIKA: Jurnal Teknik Energi Elektrik, Teknik Telekomunikasi, & Teknik Elektronika**

ISSN(p): 2338-8323 | ISSN(e): 2459-9638 | Vol. 12 | No. 4 | Halaman 1023 - 1037
DOI : http://dx.doi.org/10.26760/elkomika.v12i4.1023 Oktober 2024

# Detection Of Land Drought Using Landsat Imagery On The Google Earth Engine Platform For Forest Fire Mitigation

**HARY NUGROHO, DEWI KANIA SARI, THORIQ BAIHAQI**

Institut Teknologi Nasional Bandung, Indonesia
Email: hary@itenas.ac.id

*Received* 1 September 2024 **|** *Revised* 30 September 2024 **|** *Accepted* 30 Oktober 2024

## ABSTRAK

*Kekeringan yang diperparah oleh El Niño dan pemanasan global sering kali mejadi pemicu terjadinya kebakaran hutan di Sumatra dan Kalimantan, Indonesia, yang berdampak pada ekosistem dan masyarakat setempat. Studi ini menggunakan Temperature Vegetation Dryness Index (TVDI) yang menggabungkan Land Surface Temperature (LST) dan Normalized Difference Vegetation Index (NDVI) di platform Google Earth Engine (GEE) untuk mendeteksi area rawan kekeringan dengan cepat dan akurat. Analisis dilakukan dengan data satelit Landsat 8 dari musim kemarau tahun 2022 dan 2023 di Kabupaten Kubu Raya, Kalimantan Barat. Peta kekeringan yang dihasilkan mengidentifikasi hotspot di wilayah tengah, dengan validasi data kebakaran hutan BRIN mencapai akurasi 97%. Metode ini memberikan wawasan yang berharga bagi pemerintah daerah, memungkinkan pengambilan keputusan kebijakan yang lebih baik dan membantu pencegahan kebakaran lebih awal, meskipun terdapat kendala tutupan awan selama musim kemarau.*

***Kata kunci**: TVDI, LST, NDVI, GEE, Kebakaran Hutan*

## ABSTRACT

*Exacerbated by El Niño and global warming, drought often precedes forest fires in Sumatra and Kalimantan, Indonesia, impacting local ecosystems and communities. This study utilizes the Temperature Vegetation Dryness Index (TVDI), combining Land Surface Temperature (LST) and Normalized Difference Vegetation Index (NDVI) data on the Google Earth Engine (GEE) platform to detect drought-prone areas quickly and accurately. Analysis was performed using Landsat 8 satellite data from the 2022 and 2023 dry seasons in Kubu Raya Regency, West Kalimantan. The generated drought map identified central region hotspots, with validation using BRIN's forest fire data, achieving 97% accuracy. This method's high reliability offers valuable insights for local governments, enabling better policy decisions and aiding early fire prevention measures despite challenges like frequent cloud cover during the dry season.*

***Keywords**: TVDI, LST, NDVI, GEE, Forest Fire*

## 1. INTRODUCTION

Drought is a natural disaster that needs to be closely monitored, as it is often a precursor to forest fires. Climate change, which includes decreased rainfall, increased temperatures, and more frequent droughts, has significantly contributed to the rise in forest fires, particularly during the dry season. The El Niño phenomenon and global warming worsen this problem. Additionally, human activities contribute to forest fires **(Simioni et al., 2020)**. In Indonesia, the Head of the National Disaster Management Agency (BNPB) has indicated that most forest fires are caused by human actions **(Nugroho, 2019)**. Despite many mitigation efforts, forest fires continue to occur. According to the **Indonesian Ministry of Environment and Forestry (2023)**, forest fires in 2023 have affected 994,313 hectares with 10,673 hotspots.

Forest fires severely impact the atmosphere, soil ecology, biodiversity, and human health in forested areas **(Mutthulakshmi et al., 2020)**. Therefore, creating fire vulnerability maps is crucial, as these maps can identify potential risks and anticipate their consequences on social and environmental infrastructure **(Ghorbanzadeh et al., 2019)**. Agencies such as the Regional Disaster Management Agency (BPBD), the National Search and Rescue Agency (BASARNAS), and other relevant organizations need early information to implement preventive measures promptly, thereby limiting the spread of forest and land fires. Given the challenging accessibility in remote areas of islands like Sumatra and Kalimantan, timely delivery of drought data to relevant parties is critical, as they need time to reach severely affected areas.

Drought maps are valuable. They can reduce the vulnerability of forests to fires and enhance the decision-making process for ecological disaster mitigation **(Prayoga & Koestoer, 2021)**. These maps can be created using Geographic Information Systems (GIS) and remote sensing (RS) technologies or their integration **(Ghorbanzadeh et al., 2019)**. Several studies have explored the impact of these factors on forest fire susceptibility (FFS) mapping and drought index calculation algorithms. Methods have been developed to monitor and detect drought in specific areas, one of which uses the Temperature Vegetation Dryness Index (TVDI). TVDI values are derived from two parameters, the Normalized Difference Vegetation Index (NDVI) and Land Surface Temperature (LST), which can be extracted from Landsat 8 spectral data. Among several drought indices derived from remote sensing data, NDVI combined with LST provides a strong correlation. This information is valuable for identifying agricultural drought **(Li et al., 2024)** and monitoring plant and crop water status. When plotted, NDVI and LST create a trapezoidal space representing the spatial relationship between LST and NDVI.

Research indicates that TVDI is quite effective for drought assessment in grassland or crop areas, but its accuracy decreases in forested regions **(Przeździecki et al., 2023)**. TVDI is influenced by local biophysical conditions, which directly affect remote sensing reflectance and the resulting index values. However, TVDI can differentiate climate variability **(Alfarizi et al., 2022)**. TVDI reflects a mixed signal between soil moisture under trees and leaf water content **(Zare et al., 2020)**. According to **Holzman et al. (2014)**, TVDI should be calculated in areas with heterogeneous vegetation cover. TVDI values depend on vegetation type and density, being lower in densely vegetated regions compared to bare or moderately vegetated areas, primarily due to evaporative cooling effects **(Przeździecki et al., 2023)**.

Remote sensing has become a widely utilized tool for assessing drought, with satellite imagery commonly applied to examine drought's spatial and temporal patterns and evaluate its intensity. Over the years, remote sensing systems have amassed vast datasets. Recently, data collection has accelerated with numerous space- and airborne sensors offering various spectral, spatial, temporal, and radiometric qualities. This trend will likely grow as open-access remote sensing data and advancements in sensor technology, image processing, and computer vision become more prevalent. However, the immense volume of data makes it challenging to analyze using standard desktop software and computing resources. To overcome this, Google developed the Google Earth Engine (GEE) cloud platform to facilitate large-scale data analysis. GEE supports extensive geospatial data processing and long-term environmental assessments, proving highly effective across numerous fields since its launch in 2010 **(Amani et al., 2020)**.

Since its launch, GEE has been utilized in various applications such as vegetation assessment, land cover change detection, and flood mapping. Using the Temperature Vegetation Dryness Index (TVDI) on GEE is an effective approach for monitoring drought as part of forest fire mitigation strategies. This platform simplifies data handling, enabling rapid exploration of global drought patterns over time and space. With its adaptable spatiotemporal analysis capabilities, GEE empowers users to efficiently evaluate drought impacts **(Pham & Tran, 2021)**.

This study will identify drought areas using the TVDI index, LST and NDVI data processed on the GEE platform using Landsat 8 satellite imagery in Kuburaya Regency, West Kalimantan, Indonesia using Landsat 8 data from 2022 and 2023 dry seasons. With very rapid computation times, this platform is well-suited for geospatial analysis in evaluating drought phenomena in Indonesia. With Landsat's 16-day acquisition period, updates can be made every 16 days. If a faster update period is required, the data can be supplemented with Sentinel-2A satellite imagery with a 5-day acquisition period. Thus, information on areas that have reached extreme drought can be quickly communicated to relevant parties.

## 2. MATERIAL AND METHODS

### 2.1 Study Area

The research area falls within the administrative region of Kubu Raya Regency, West Kalimantan Province, geographically situated at coordinates 108° 35' – 109° 58' East Longitude and 0° 44' North Latitude – 1° 01' South Latitude, see Figure 1. The regency covers an area of 6,985.20 km², 4,785 km² of land, and 2,197 km² of sea, with 39 small islands. The terrain is predominantly flat, with slopes of 0 – 3% covering 792,320 hectares (98%), 3 – 15% covering 7,205 hectares and above 40% covering 850 hectares. According to the Schmit & Ferguson classification, the climate in Kubu Raya falls under Climate Type A, characterized as very wet, with monthly rainfall exceeding 100 mm and an average annual rainfall of approximately 3000 mm. The maximum average temperature of 33.4°C occurs in May, and the minimum average temperature of 22.5°C occurs in August **(Pemerintah Kabupaten Kubu Raya, 2024)**.

Kubu Raya Regency is one of the areas prone to forest and land fires, especially during the dry season. This vulnerability is partly due to the predominance of organic/peat soils, which are more flammable. Land use in Kubu Raya is primarily vegetative, including forest areas, plantations, and shrubs. In this area, forest fires result from natural causes and are driven by human activities. These activities include land clearing and preparation by plantation owners, farmers, the forestry sector, and the expansion of transmigration settlements **(Muharrama & Widjonarko, 2023)**.


**Figure 1. Kubu Raya Regency, West Kalimantan Province**

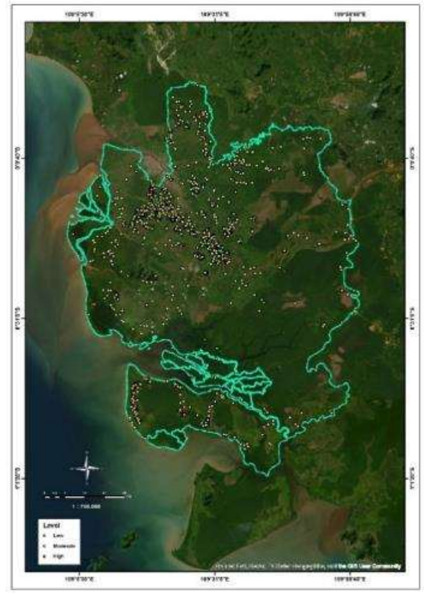

**Figure 2. High forest fire vulnerability at Kubu Raya Regency, West Kalimantan Province**

## 2.2 Forest Fire Inventory

Forest fire data (hotspots) were obtained based on the identification conducted by BRIN. This identification utilized the Terra and Aqua satellites equipped with MODIS sensors on channels 21 and 22, the S-NPP (Suomi-National Polar-orbiting Partnership) and NOAA-20 satellites equipped with sensors on channel I4, and the Landsat 8 satellite equipped with the OLI sensor on channel 7. The hotspot information is then uploaded to the website https://hotspot.brin.go.id/. During the 2022-2023 period, 2,161 hotspots were recorded, of which 40 were identified as high-probability occurrences, 2,019 as moderate, and 102 as low. This study used the hotspot data to validate the classification results of areas with high forest fire vulnerability, see Figure 2.

## 2.3 Google Earth Engine (GEE)

Google Earth Engine (GEE) is a powerful cloud platform for extensive geospatial data analysis and environmental monitoring. It provides access to an extensive repository of satellite imagery, including data from sources like Landsat, MODIS, and Sentinel, allowing researchers to perform advanced spatial analyses without requiring high-end computing resources. GEE's ability to process vast datasets in real-time makes it particularly suitable for assessing environmental changes, such as drought monitoring, land cover change, and vegetation dynamics. With its user-friendly interface and robust scripting capabilities, GEE simplifies the integration of multiple data types, enabling users to conduct complex geospatial analyses efficiently and effectively.

For assessing land drought, GEE offers a comprehensive data catalog and powerful tools that facilitate efficient calculation of indices like the Normalized Difference Vegetation Index (NDVI) and Land Surface Temperature (LST), which are crucial for analyzing drought conditions. The Temperature Vegetation Dryness Index (TVDI), a crucial metric in drought studies, can be derived by combining NDVI and LST data within the GEE environment. The platform's scripting interface allows researchers to automate processes, conduct regression analyses, and generate spatial maps of drought indices with high accuracy and efficiency. The use of GEE not only accelerates the analysis process and enhances the reproducibility and scalability of drought assessments, making it an ideal choice for environmental monitoring and decision-making.

## 2.4 Data Resources

Google Earth Engine (GEE) provides an extensive library of satellite imagery curated by Google, with each dataset having a unique Image Collection and ID available through the GEE catalog on their website (https://earthengine.google.com/datasets/). This platform grants access to a vast range of multi-source satellite data and high-performance computing resources, enabling quick and flexible processing of satellite images. Landsat 8, available on GEE since the satellite's 2013 launch, has a 16-day revisit period and resolutions that vary from 15 meters (panchromatic) to 100 meters (thermal infrared), with multispectral imagery typically at 30 meters. Users can access all Landsat 8 datasets, including Tier 1, Tier 2, raw scenes, top-of-atmosphere (TOA), and surface reflectance (SR) data, with thermal bands resampled to a 30-meter spatial resolution.

Using JavaScript or Python code on the GEE cloud platform, Landsat images can be easily resampled to a common spatial resolution, such as 30 meters, and transformed into a uniform map projection, like Geographic Lat/Lon (Xie et al., 2019). This capability simplifies the processing of multi-source and multitemporal satellite imagery, removing the need for labor-intensive tasks like mosaicking, registration, projection conversion, and resampling. Table 1 presents the Landsat data used in this study. The Landsat 8 imagery selected for this research was captured in 2022 and 2023 and includes Tier 1 (T1) data, which offers the best radiometric and positional accuracy and is recommended by the USGS for time-series analysis. All images used in this study have less than 30% cloud cover.

**Tabel 1. List of products in the GEE catalog used in the study**

| ID | Used Bands | Spatial Resolution | Duration |
|---|---|---|---|
| LANDSAT/LC08/C02/T1 | Tier 1, SR | 30 m | 2022-05-01 until 2022-06-01 |
| LANDSAT/LC08/C02/T1 | Tier 1, SR | 30 m | 2023-05-01 until 2023-06-01 |
| LANDSAT/LC08/C02/T1_TOA | Tier 1, TOA | 100 m, resampled to 30 m. | 2022-05-01 until 2022-06-01 |
| LANDSAT/LC08/C02/T1_TOA | Tier 1, TOA | 100 m, resampled to 30 m. | 2023-05-01 until 2023-06-01 |

Notes: SR: Surface Reflectance, TOA: Top Of Atmosphere

## 2.5 Methodology

The data processing steps are illustrated in the flowchart in Figure 3. The initial step involves radiometric calibration, where digital number (DN) pixel values are converted to brightness temperature (T). Additionally, DN is converted to radiance and reflectance. Following this, atmospheric correction is applied to bands 4 and 5, converting top-of-atmosphere radiance (LTOA) and reflectance (ρTOA) to bottom-of-atmosphere radiance (LBOA) and reflectance (ρBOA). The corrected bands 4 and 5 combine to produce a new image representing the vegetation’s greenness.

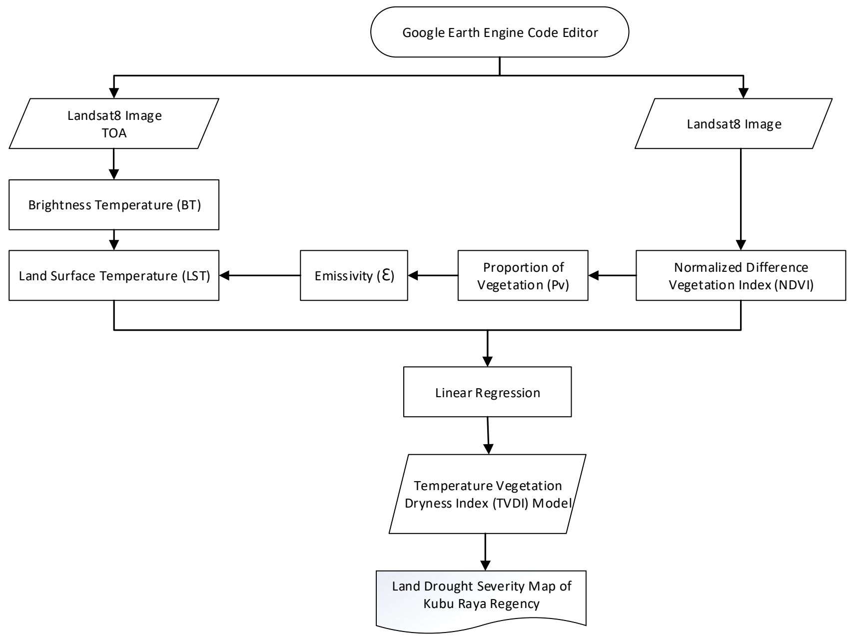


**Figure 3. Methodology**

The next step is to calculate the proportion of vegetation (Pv) to determine the emissivity parameter using the processed NDVI values. Land surface emissivity is calculated to obtain the emissivity value (ε) used in the formula for calculating land surface temperature. Land Surface Temperature (LST) is derived using a formula to obtain the temperature distribution from Landsat 8 satellite images. Linear regression is employed to determine the parameters for the TVDI equation by analyzing the relationship between NDVI and LST values. The Temperature Vegetation Dryness Index (TVDI) is then used to map land dryness distribution from Landsat 8 imagery, indicating the dryness level in the observed area and serving as an indicator of potential forest fire risk.

## 2.6 Land Surface Temperature (LST)

LST indicates the temperature of the Earth's surface as observed from space, offering essential data about the land's thermal condition **(Li et al., 2023)**. It is a crucial parameter for understanding the surface energy balance and environmental conditions, making it an essential factor in drought detection studies. LST represents the balance between incoming solar radiation and outgoing thermal radiation, and is strongly affected by surface characteristics such as vegetation cover, soil moisture, and land use. In drought conditions, LST typically increases due to reduced evapotranspiration, making it a valuable indicator for assessing the extent and severity of droughts **(Cheng et al., 2023)**.

LST is commonly derived from satellite imagery's thermal infrared (TIR) bands, such as those captured by the Landsat series **(Guha et al., 2020)**. The process involves converting the digital numbers from the thermal bands into at-sensor radiance and then calculating brightness temperature using Planck's Law **(Zare et al., 2020)**. Surface emissivity corrections are applied to obtain accurate LST, accounting for the differences in heat emission across various land cover types. Surface emissivity is a crucial parameter, as it adjusts the brightness temperature to reflect the actual surface temperature **(Hulley & Lluis Perez-Planells, 2024)**, compensating for the Earth's surface not emitting radiation as a perfect blackbody. The corrected LST data provides a spatially detailed representation of surface temperatures, which can highlight areas of thermal stress associated with drought when combined with vegetation indices.

The retrieval of LST from Landsat data involves several steps, starting with converting thermal radiance to brightness temperature, followed by adjustments for surface emissivity. The brightness temperature (BT) is determined using the following equation **(Zare et al., 2020)**:

$$BT = \frac{K_2}{ln\left(\frac{K_1}{L_\lambda}+1\right)} \quad (1)$$

$K_1$ and $K_2$ are calibration constants specific to the Landsat sensor, and λ is the spectral radiance. After calculating the BT, an emissivity correction is applied to estimate the LST using:

$$LST = \frac{BT}{1+(\lambda.BT/\rho).ln(\epsilon)} \quad (2)$$

In this equation, λ represents the wavelength of emitted radiance, ρ is a constant, and ϵ denotes the surface emissivity value. This correction is important because emissivity varies across different land cover types, affecting the precision of LST measurements.

LST plays a crucial role in the Temperature Vegetation Dryness Index (TVDI), which combines with vegetation indices like NDVI to assess surface dryness. By analyzing the spatial distribution of LST, researchers can identify hotspots of elevated temperatures that correlate with drought-affected areas. Higher LST values often correspond to reduced soil moisture and vegetation stress, critical indicators of drought conditions. Thus, LST serves as a vital input in drought monitoring, enabling the identification of areas experiencing thermal stress due to prolonged dry spells.

## 2.7 Normalized Difference Vegetation Index (NDVI)

NDVI is a commonly used remote sensing index that assesses vegetation health by calculating the difference between near-infrared (NIR) and red light, spectral bands typically captured by satellite sensors like Landsat, MODIS, and Sentinel. The NDVI is computed using the following formula **(Zare et al., 2020)**:

$$NDVI = \frac{NIR-Red}{NIR+R} \quad (3)$$

NIR refers to the near-infrared reflectance, while red represents the reflectance of red light. This formula generates values between -1 and +1, with higher values indicating healthy, dense vegetation, and lower values corresponding to sparse vegetation or non-vegetated areas such as water, bare soil, or urban surfaces. In the context of drought monitoring, NDVI is valuable for assessing vegetation conditions and estimating Land Surface Temperature (LST). NDVI serves as an indirect indicator of surface characteristics; areas with high NDVI values generally correspond to healthy vegetation with lower temperatures, while areas with low NDVI values indicate sparse vegetation or bare soil with higher temperatures. By establishing a relationship between NDVI and LST, it is possible to infer surface moisture conditions, as areas with low vegetation cover tend to exhibit higher surface temperatures due to increased exposure to solar radiation. This relationship makes NDVI a crucial parameter in understanding the spatial distribution of temperature variations across different land cover types, ultimately aiding in drought detection and analysis.

## 2.8 Temperature Vegetation Dryness Index (TVDI)

The TVDI is a drought index that combines Land Surface Temperature (LST) and vegetation cover, often represented by the Normalized Difference Vegetation Index (NDVI), to evaluate surface moisture levels and determine drought severity. TVDI is particularly effective in identifying the spatial variability of soil moisture by combining thermal and vegetation information derived from satellite imagery, such as Landsat, MODIS, or Sentinel data. The index is based on the "triangle" or "trapezoid" space between LST and NDVI, where the lower edge represents wet conditions, and the upper edge represents dry conditions. TVDI is calculated using the formula **(Zare et al., 2020)**:

$$TVDI = \frac{LST - LST_{min}}{LST_{max} - LST_{min}} \tag{4}$$

where LST is the observed land surface temperature, and LSTmin and LSTmax represent the minimum and maximum temperatures corresponding to a given NDVI value, respectively. High TVDI values indicate dry surface conditions, while low values suggest wetter conditions. This relationship makes TVDI a valuable tool for monitoring drought, providing a spatially detailed view of moisture stress on vegetation and soil. By effectively integrating thermal and vegetation data, TVDI enhances the ability to detect and analyze drought conditions over large areas, making it a critical index for environmental monitoring and management.

### 2.9 Wet and dry edges by linear regression

The Temperature Vegetation Dryness Index (TVDI) relies on identifying the wet and dry edges in the scatterplot of Land Surface Temperature (LST) against the Normalized Difference Vegetation Index (NDVI). This scatterplot forms a triangular or trapezoidal space where the wet and dry edges define the minimum and maximum LST values corresponding to varying vegetation conditions, indicating surface moisture status. The wet edge represents the lower boundary of the scatterplot, where surface conditions are moist, leading to lower LST values for a given NDVI. In contrast, the dry edge represents the upper boundary, where surface conditions are dry, resulting in higher LST values for the same NDVI. These edges are determined through linear regression analysis: the wet edge is modelled by fitting a line to the minimum LST values along the NDVI axis, and the dry edge is modelled by fitting a line to the maximum LST values.

## 3. RESULT AND DISCUSSION

The land surface temperature mapping in Kuburaya Regency, West Kalimantan, was conducted using Landsat 8 imagery and Google Earth Engine (GEE). The analysis began with the Top of Atmosphere (TOA) correction, converting digital numbers to reflectance or radiance using Landsat 8 metadata. Brightness Temperature was then calculated, assuming it represents the TOA radiance. Key parameters used in GEE included Radiance_Mult_Band_10 (0.0003342), Radiance_Add_Band_10 (0.1), and Band 10 for Qcal, while Brightness Temperature utilized constants K2 (1321.08) and K1. The processed data were used to calculate Land Surface Temperature (LST) in GEE, followed by temperature classification to create a visual map: 18-21°C (dark green), 21-24°C (light green), 24-27°C (yellow), 27-30°C (orange), and 30-35°C (red). This classification reveals temperature variations, with elevated temperatures primarily found in urban and deforested areas. This highlights the effect of land use changes on surface heating. The resulting map showcases notable spatial differences in LST, emphasizing the role of land cover in shaping local temperature patterns, see Figure 4a and 4b.

The vegetation index in Kuburaya Regency was assessed using Landsat 8 TOA data, specifically utilizing Band 5 (NIR) and Band 4 (RED). Band 5 captures near-infrared light, reflecting information about the amount and condition of vegetation, while Band 4 detects light reflected from bare surfaces such as soil, rocks, and non-living vegetation. The vegetation index was computed using the formula (B5-B4)/(B5+B4 ) within the Google Earth Engine platform. The analysis revealed that in 2022, NDVI values ranged from -0.61939 to 0.864248, while in 2023, the range was -0.595783 to 0.852735. The average NDVI was -1.395321203 in 2022 and -1.431284545 in 2023, showing a slight change between the two years, see Figure 5a and 5b. NDVI values were classified as follows: -1.0 to -0.3 indicates non-vegetation, -0.3 to 0.25 indicates low vegetation, 0.25 to 0.4 indicates moderate vegetation and 0.4 to 1.0 indicates high vegetation (Pietersz et al., 2024).

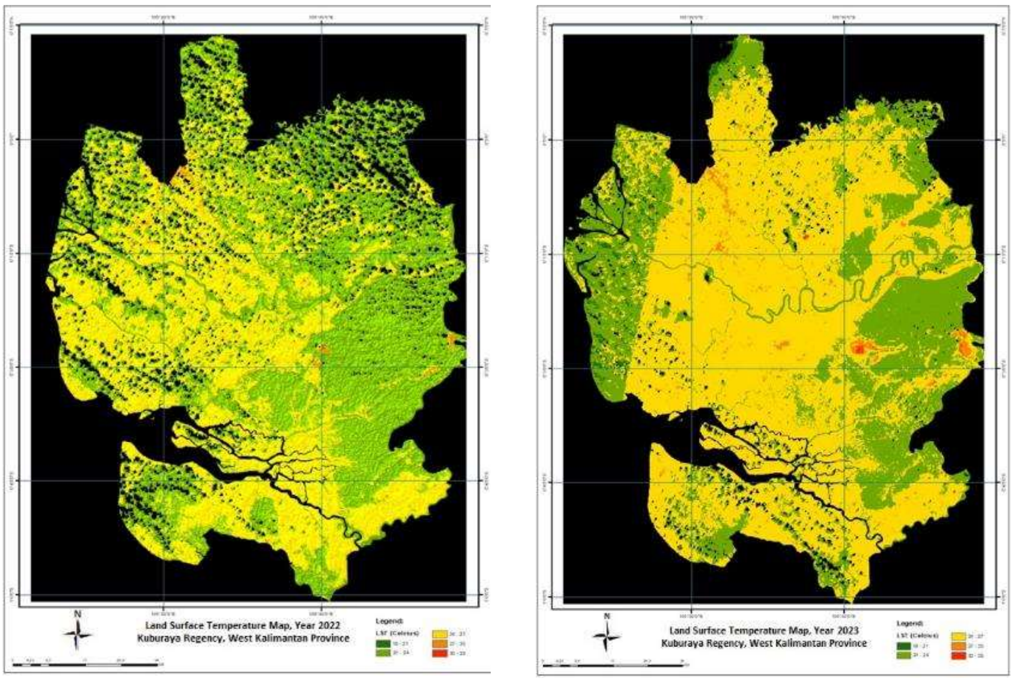


**(a)** **(b)**

**Figure 4. Land Surface Temperature year 2022 and 2023**

The Temperature Vegetation Dryness Index (TVDI) model utilizes the triangular relationship between NDVI and land surface temperature (LST) to determine soil moisture levels. Plotting NDVI on the x-axis against LST on the y-axis forms a triangular pattern, which identifies the wet (LSTmin) and dry (LSTmax) edges through regression lines. The equations for these lines are defined as

$$y = a + \beta x \quad (5)$$

$y$ = dependent variable (LST), $a$ = intercept, $\beta$ = slope, and $x$ = independent variable (NDVI). The regression values of LSTmin and LSTmax are crucial in this study, as they provide the necessary parameters for calculating the TVDI, which relies on the linear regression lines of the wet and dry edges derived from random NDVI and LST sample points. Figures 6a and 6b display the regression lines for wet (y = 2.7139 x + 21.469) and dry edges (y = -3.0648 x + 26.791) based on NDVI and LST data for May-June 2022. Similarly, Figures 6c and 6d show the regression lines for May-June 2023, with the wet edge line (y = 3.228 x + 21.062) and dry edge line (y = -3.7816 x + 27.595).

The drought index mapping in Kabupaten Kuburaya was derived using several parameters. The first parameter is Land Surface Temperature (LST), which produces an output image representing temperature values in degrees Celsius. The second parameter is the Normalized Difference Vegetation Index (NDVI), which generates an image with values ranging from -1 to 1, reflecting vegetation index levels. The third parameter involves regression values for wet and dry boundaries created from the scatter of randomly selected sample points. These boundaries are separated based on data, with NDVI values on the X-axis and LST values on the Y-axis. These two regression lines (NDVI and LST) are used in the TVDI modeling calculations. The LST and NDVI images were obtained from prior processing steps, while the wet and dry boundary regression values for 2022 were $y = 2.7139x + 21.469$ (damp) and $y = -3.0648x + 26.791$ (dry). In 2023, the wet boundary regression was $y = 3.228x + 21.062$, and the dry boundary was $y = -3.7816x + 27.595$.

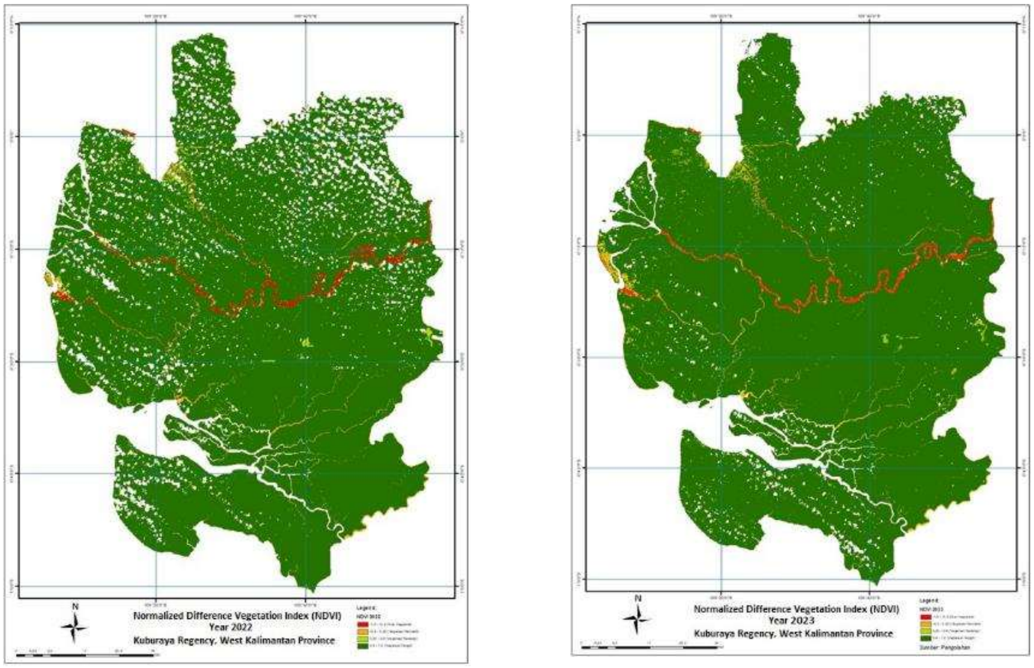


**(a)** **(b)**

**Figure 5. Normalized Difference Vegetation Index (NDVI) year 2022 and 2023**

These three parameters—LST, NDVI, and regression values for wet and dry boundaries—were substituted into the TVDI formula: (LST - LSTmin) / (LSTmax - LSTmin), where LSTmax = a + b * NDVI and LSTmin = c + d * NDVI. After TVDI modeling, classification was conducted using a range of 0 to 1, where 0 – 0.20 indicates wet, 0.21 – 0.40 slightly wet, 0.41 – 0.60 moderate, 0.61 – 0.80 somewhat dry, and 0.81 – 1.00 dry (Sandholt et al., 2002).

Figures 7a and 7b display drought conditions in Kabupaten Kuburaya. In both figures, dry areas (red) are predominantly found in the west and south, while the eastern region is primarily categorized as wet (green). However, the extent of drought-affected areas in Figure 7b more significant. Black areas represent cloud cover, which was removed during initial processing. Based on this analysis, the TVDI drought index map for Kabupaten Kuburaya is presented below. The results of the land dryness map using the TVDI model, which incorporates LST and NDVI parameters, indicate that the Kabupaten Kuburaya area was predominantly covered by red zones in May-June 2022, see Figure 7a, signifying extensive dry land conditions. Similarly, in May-June 2023, the region was also dominated by red zones, indicating widespread dry conditions, see Figure 7b. The primary cause of these dry conditions in Kabupaten Kuburaya during both years was the peak of the dry season in 2022 and 2023.

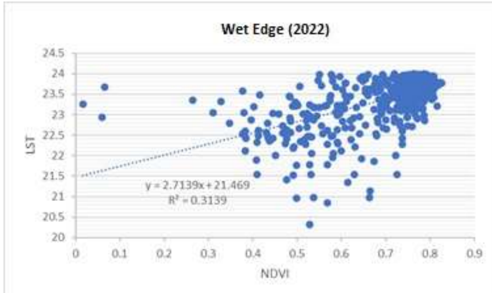


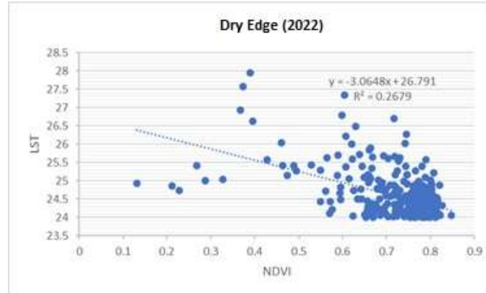


**(a)** **(b)**

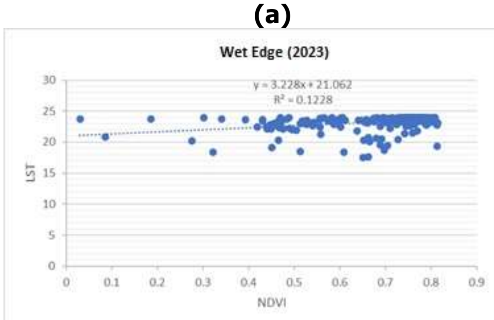


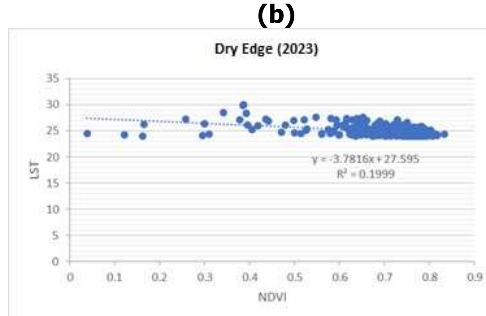


**(c)** **(d)**

**Figure 6. Regression Lines for Wet and Dry Edge, year 2022 and 2023**

To validate the drought conditions identified by the TVDI, forest fire points from BRIN were overlaid on the drought map, see Figure 8. These fire points serve as an independent indicator of dry conditions, as forest fires are often closely associated with severe drought. The presence of fire points within areas classified as highly dry by the TVDI confirms the accuracy of the drought index in capturing actual drought occurrences on the ground. This validation step strengthens the reliability of the TVDI map, demonstrating its effectiveness in identifying drought-prone areas that correspond with observed environmental stress. The integration of forest fire data provides a practical cross-reference, ensuring that the mapped drought areas are not only theoretical but also reflect real-world conditions.

The relationship between land dryness levels and hotspot distribution data from BRIN was analyzed. In May-June 2022, the TVDI drought index identified 25 hotspots, with 19 located in dry areas (red), 2 in moderately dry areas (orange), 1 in areas with medium dryness (yellow), and 3 in cloud-covered regions. In May-June 2023, of the 44 identified hotspots, 36 were in dry areas (red), 4 in moderately dry areas (orange), 1 in medium dryness areas (yellow), and 3 in cloud-covered regions. The correspondence between the dry index (red) and hotspot locations was 76% in 2022 and 81.82% in 2023.

The analysis of the TVDI maps for Kabupaten Kuburaya reveals a consistent pattern of extensive dry land conditions during the peak of the dry season in 2022 and 2023. Both periods (May-June) were characterized by a predominance of red areas on the TVDI maps, indicating severe drought conditions. The validation with hotspot data further supports these findings, as a significant number of hotspots corresponded with dry areas identified by the TVDI. In 2022, 76% of the hotspots were located within dry zones, and this percentage increased to 81.82% in 2023. This strong correlation between TVDI drought classifications and the spatial distribution of hotspots confirms the effectiveness of TVDI as a reliable drought monitoring tool. The high incidence of drought is likely attributed to the alignment with the peak dry season, emphasizing the critical need for effective drought management strategies in the

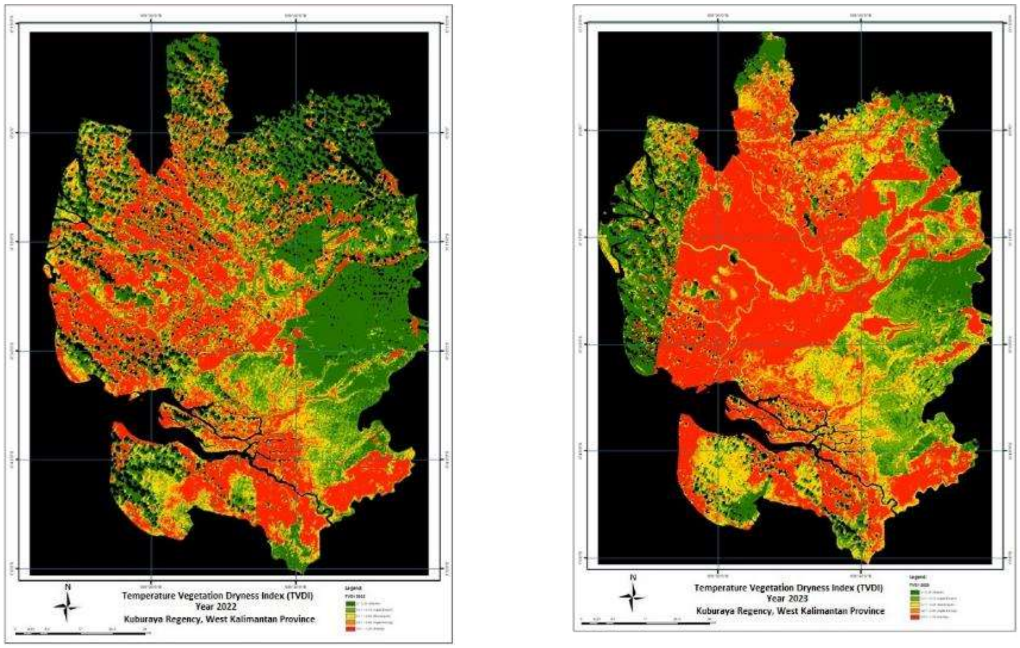


**(a)** **(b)**

**Figure 7. Temperature Vegetation Dryness Index (TVDI)**

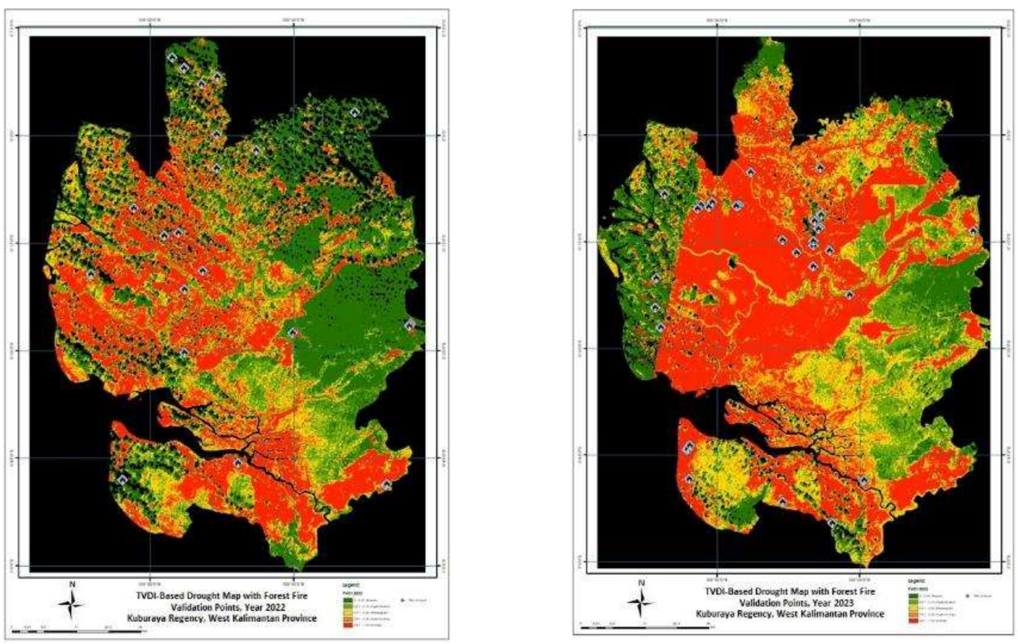


**(a)** **(b)**

**Figure 8. Validation Map**

## 4. CONCLUSION

The TVDI model's use to analyze drought conditions in Kabupaten Kubu Raya has demonstrated its effectiveness as a tool for monitoring land dryness. The results from the TVDI maps for May-June 2022 and 2023 indicate a significant prevalence of dry areas, confirming the region's vulnerability to drought during the peak dry season. The validation with hotspot data reinforces the reliability of the TVDI index, with a notable correlation between drought zones and the distribution of fire hotspots. These findings underscore the urgent need for targeted drought management strategies and policies to mitigate the impact of drought on agricultural and ecological systems in Kabupaten Kuburaya. Future research should focus on integrating additional environmental variables to enhance the predictive capability of drought assessments in this region.

## REFERENCES


Alfarizi, I. A. G., Herlambang, G. A., Hartono, R., Sucahyo, H. R., Wiwoho, B. S., & Astuti, I. S. (2022). Drought Indices to Map Forest Fire Risks in Topographically Complex Mountain Landscapes. *KnE Social Sciences*, *2022*, 197–209. https://doi.org/10.18502/kss.v7i16.12167

Amani, M., Ghorbanian, A., Ahmadi, S. A., Kakooei, M., Moghimi, A., Mirmazloumi, S. M., Moghaddam, S. H. A., Mahdavi, S., Ghahremanloo, M., Parsian, S., Wu, Q., & Brisco, B. (2020). Google Earth Engine Cloud Computing Platform for Remote Sensing Big Data Applications: A Comprehensive Review. *IEEE Journal of Selected Topics in Applied Earth Observations and Remote Sensing*, *13*, 5326–5350. https://doi.org/10.1109/JSTARS.2020.3021052

Cheng, L., Liu, S., Mo, X., Hu, S., Zhou, H., Xie, C., Nielsen, S., Grosen, H., & Bauer-Gottwein, P. (2023). Assessing the Potential of 10-m Resolution TVDI Based on Downscaled LST to Monitor Soil Moisture in Tang River Basin, China. *Remote Sensing*, *15*(3). https://doi.org/10.3390/rs15030744

Ghorbanzadeh, O., Blaschke, T., Gholamnia, K., & Aryal, J. (2019). Forest fire susceptibility and risk mapping using social/infrastructural vulnerability and environmental variables. *Fire, 2*(3), 1–27. https://doi.org/10.3390/fire2030050

Guha, S., Govil, H., Gill, N., & Dey, A. (2020). Analytical study on the relationship between land surface temperature and land use/land cover indices. *Annals of GIS*, *26*(2), 201–216. https://doi.org/10.1080/19475683.2020.1754291

Holzman, M. E., Rivas, R., & Piccolo, M. C. (2014). Estimating soil moisture and the relationship with crop yield using surface temperature and vegetation index. *International Journal of Applied Earth Observation and Geoinformation*, *28*(1), 181–192. https://doi.org/10.1016/j.jag.2013.12.006

Hulley, G., & Lluis Perez-Planells. (2024). *Terminology in thermal infrared remote sensing of natural surfaces. Land Product Validation Subgroup*. Retrieved from https://lpvs.gsfc.nasa.gov/LSTE/LSTE_home.html#:~:text=Land Surface Emissivity Definition,Units%3A Dimensionless.

Li, Y., Wang, X., Wang, F., Feng, K., Li, H., Han, Y., & Chen, S. (2024). Temporal and Spatial Characteristics of Agricultural Drought Based on the TVDI in Henan Province, China. *Water (Switzerland)*, *16*(7). https://doi.org/10.3390/w16071010

Li, Z. L., Wu, H., Duan, S. B., Zhao, W., Ren, H., Liu, X., Leng, P., Tang, R., Ye, X., Zhu, J., Sun, Y., Si, M., Liu, M., Li, J., Zhang, X., Shang, G., Tang, B. H., Yan, G., & Zhou, C. (2023). Satellite Remote Sensing of Global Land Surface Temperature: Definition, Methods, Products, and Applications. *Reviews of Geophysics*, *61*(1), 1–77. https://doi.org/10.1029/2022RG000777

Muharrama, D., & Widjonarko, W. (2023). Risiko Bencana Kebakaran Hutan dan Lahan Gambut di Kabupaten Kubu Raya, Provinsi Kalimantan Barat. *Teknik PWK (Perencanaan Wilayah Kota)*, *12*(2), 160–170. https://doi.org/10.14710/tpwk.2023.32816

Mutthulakshmi, K., Wee, M. R. E., Wong, Y. C. K., Lai, J. W., Koh, J. M., Acharya, U. R., & Cheong, K. H. (2020). Simulating forest fire spread and fire-fighting using cellular automata. *Chinese Journal of Physics*, *65*(April), 642–650. https://doi.org/10.1016/j.cjph.2020.04.001

Nugroho, S. P. (2019). *99% Penyebab Kebakaran Hutan dan Lahan Adalah Ulah Manusia. BNPB.Go.Id.* Retrieved from https://bnpb.go.id/99-penyebab-kebakaran-hutan-dan-lahan-adalah-ulah-manusia

Pemerintah Kabupaten Kubu Raya. (2024). *Geografi*. Humas Kabupaten Kubu Raya. Retrieved from https://prokopim.kuburayakab.go.id/page/geografi

Pham, H. T. T., & Tran, H. T. (2021). Application of Remote Sensing Imagery and Algorithms in Google Earth Engine platform for Drought Assessment. *Journal of Mining and Earth Sciences, 62*(3), 53–67. https://doi.org/10.46326/jmes.2021.62(3).07

Pietersz, J. H., Pribadi, R., & Pentury, R. (2024). Estimasi Tutupan Kanopi Berdasarkan NDVI dan Kondisi Tutupan Tajuk Pada Ekosistem Mangrove Negeri Passo, Teluk Ambon Dalam. *Jurnal Kelautan Tropis*, *27*(2), 197–208. https://doi.org/10.14710/jkt.v27i2.22090

Prayoga, M. B. R., & Koestoer, R. H. (2021). Improving Forest Fire Mitigation in Indonesia: A Lesson from Canada. *Jurnal Wilayah dan Lingkungan*, *9*(3), 293–305. https://doi.org/10.14710/jwl.9.3.293-305

Przeździecki, K., Zawadzki, Jdeteksi . J., Urbaniak, M., Ziemblińska, K., & Miatkowski, Z. (2023). Using temporal variability of land surface temperature and normalized vegetation index to estimate soil moisture condition on forest areas by means of remote sensing. *Ecological Indicators*, *148*(March), 0–3. https://doi.org/10.1016/j.ecolind.2023.110088

Sandholt, I., Rasmussena, K., & Andersen, J. (2002). A simple interpretation of the surface temperature/vegetation index space for assessment of surface moisture status. *Remote Sensing of Environment*, *79*(2–3), 213–224. https://doi.org/10.1016/s0034-4257(01)00274-7

Simioni, G., Marie, G., Davi, H., Paul, N. M.-S., & Huc, R. (2020). Natural forest dynamics have more influence than climate change on the net ecosystem production of a mixed Mediterranean forest. *Ecological Modelling*, *416*(108921). https://doi.org/10.1016/j.ecolmodel.2019.108921

Xie, S., Liu, L., Zhang, X., Yang, J., & Chen, X. (2019). Automatic Land-Cover Mapping using Landsat Time-Series Data based on Google Earth Engine. *Remote Sensing, 11*(3023), 1–20. https://doi.org/10.3390/rs11243023

Zare, M., Drastig, K., & Zude-Sasse, M. (2020). Tree water status in apple orchards measured by means of land surface temperature and vegetation index (LST-NDVI) trapezoidal space derived from landsat 8 satellite images. *Sustainability (Switzerland)*, *12*(1), 1–19. https://doi.org/10.3390/SU12010070